



Original Research Article

Synthesis, Characterization and Thermal Properties of Some Acrylamide and *Cis*-2-Butene-1, 4-Diol Copolymers Using CAN as Initiator

Mahir A. Jalal * , Enas A. Nasir , Zainab J. Sweah , Alyaa Abdulhasan Abdulkarem , Haider Abdulelah

Department of Polymer Technology, Polymer Research Center, University of Basrah, Basrah, Iraq

ARTICLE INFO

Article history

Submitted: 2024-07-10

Revised: 2024-08-26

Accepted: 2024-09-11

ID: [AJCA-2408-1634](https://doi.org/10.48309/AJCA.2025.472480.1634)

DOI: 10.48309/AJCA.2025.472480.1634

KEYWORDS

Thermal properties

Cis-2-butene-1,4-diol copolymers

Thermal stability

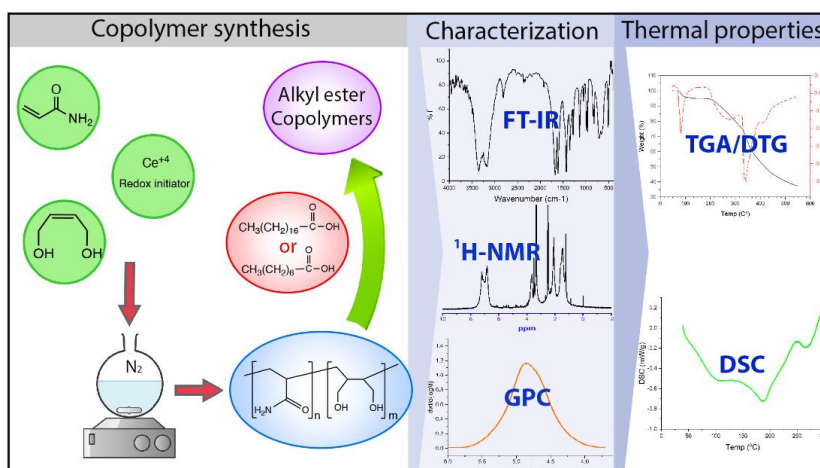
Inhibitor

Copolymer synthesis

ABSTRACT

In this study, poly (acrylamide-*co*-*cis*-2-butene-1, 4-diol) was synthesized by polymerization of various molar ratios of acrylamide and *cis*-2-butene-1, 4-diol using ceric ammonium nitrate (CAN) as redox initiator. The copolymer then has been modified through incorporating of linear alkyl ester chains (C_8 and C_{18}) into copolymer by esterification reaction as melts using pTsoH as catalyst. Resulting copolymers were purified and characterized by FT-IR, NMR, and GPC. All analyses indicate that *cis*-2-butene-1,4-diol has the ability to act as both a monomer and a reducing agent which confirms the validity of the proposed mechanism. The reaction conditions have been varied and the best yield of copolymer is 65.1% under these following optimum reaction conditions; 8 mL of CAN solution, 2.4×10^{-3} mmol of acrylamide, 19.6×10^{-3} mmol of *cis*-2-butene-1,4-diol, 6 hours reaction time, and 50 °C reaction temperature. GPC and hydroxyl number determination showed acrylamide units consist of the larger portion in the copolymer chains. Thermal characterization of copolymers was also investigated using TGA, DTG, and DSC analysis. TGA/DTG revealed multi-stage decomposition, while DSC exhibited a shift in the T_g peak after reaction with aliphatic carboxylic acids. Kinetics of thermal decomposition was also investigated using models of the Coats-Redfern and the second order of the chemical reaction was found to be more appropriate to describe the reaction model for the thermal degradation of copolymers with R^2 correlation up to 99.7%. The activation energy in the region of T_{max} also increased by adding longer alkyl ester group to the copolymer, which can contribute to the improvement of its thermal stability.

GRAPHICAL ABSTRACT



* Corresponding author: Jalal, Mahir A.

✉ E-mail: mahir.jalal@uobasrah.edu.iq

© 2025 by SPC (Sami Publishing Company)

Introduction

Ceric ammonium nitrate has a chemical formula $\text{Ce}(\text{NH}_4)_2(\text{NO}_3)_6$ and well-knowns oxidizing agent for some organic substances in the acidic media. With the aid of reducing agent, ceric ions also function as redox initiator by producing active sites or free-radicals for vinyl polymerization [1]. In this process, an oxidizing agent, Ce (IV) firstly forms a complex by reacting simply with organic substance which then dissociates unimolecularly to produce free radicals that initiate polymerization [2]. However, formation of the redox polymerization system required a lower activation energy than conventional thermal polymerization that allowing polymerization to be accomplished under milder conditions [3].

Several synthetic methodologies based on ceric ions have been developed over the past few decades and have made it possible to either prepare new polymers or increase polymer yields. Some researchers manipulated concentrations of all reaction components and found each individual Ce (VI)-redox polymerization reaction have its optimum condition [4]. N. Mzinyane [5] found low temperatures can be employed with this redox systems and increasing temperature, up to 70°C, has a positive effect on polymer yield. Jignesh H. Trivedi *et al.* [6] reported that the presence of UV light assisted oxidative polymerization along with ceric ions can optimize copolymerization of acrylonitrile onto sodium salt of partially carboxymethylated tamarind kernel powder. S. Jha *et al.* [7] exposed a mixture of acrylamide, polysaccharide, and CAN to short-term microwave radiation to initiate copolymerization onto the surface of polysaccharide. A. Yavla *et al.* [8] recently obtained polycarbazole with solid-state polymerization without solvent by imposing solid reactants to high pressure or ultrasonic waves. However, those modifications on general synthetic strategy allowed to incorporate reducing agents containing various

functional groups like alcohols [9], polyols [10], amines [11], acids [12], thiols [13], thiourea [14], and saccharides [15], each more suitable for different monomers.

Many copolymers obtained through Ce (VI)-induced redox polymerization were found to be suitable for different applications. For instance, E. Kot *et al.* [16] used CAN and 2,2'-azobis[2-methyl-N-(2-hydroxyethyl)propionamide] as oxidizing and reducing agents containing a degradable moiety, respectively, to initiate polymerization of acrylamide monomer and found that such water-soluble polymer had a potential contribution in the oil and gas industry by using it as drag reducing-agent (DRA) in water brine. T. Song *et al.* [17] polymerized acrylamide monomer in redox system of arginine and Ce (IV). The resulting polymer exhibited a gelation property used as enhanced oil recovery (EOR) treatment to control the excessive water production problem in oil industry. Utilizing Ce (VI)-redox polymerization to produce conductive polymers was also conducted by Y. Tatar *et al.* [18]. They prepared a block copolymer of polypyrrole and thienyl end-capped cyclohexanone formaldehyde resin and its chains have a conductance property via electroactive conjugated segment (polypurrole) and spacer segment (reducing agent). R. Bhosale *et al.* [19] recently developed a pH-sensitive polymeric delivery system by grafting Ghatti gum with methyl methacrylate chains using chemical oxidative polymerization initiated by CAN. An attempt to produce super water absorber biopolymer from natural sources was successfully achieved by E. Czarnecka and J. Nowaczyk [20]. They grafted starch with acrylic acid through Ce (VI)-induced redox polymerization process. The grafted chains are hydrophilic part of resulting crosslinked copolymer. Others modified hydrogels of cellulose nanofibril and made them more sustainable to elevated temperatures [21]. They initiated Ce (IV) redox polymerization of N,N-dimethylacrylamide and butyl acrylate onto

cellulose particles surface. Grafting poly (acrylamide) on cross-linked poly (4-vinyl pyridine) was also conducted using CAN as redox initiator [22]. The resulting copolymer showed a high-capacity mercury specific sorbent.

As many water-soluble monomers were synthesized within the past few decades, there is still need more researches focusing on driving these developments and monomers to produce new polymers. In this study, *cis*-2-butene-1,4-diol was used as monomer and reducing agent to produce a new water-soluble copolymer. The copolymer, then, increased its lipophilicity through introducing long chains of aliphatic hydrocarbons into backbone. Such a chemical structure is useful in producing chemicals important in petroleum industry such as pour point depressants and drag reducing agents.

Experimental

Materials

Acrylamide (98%) was supplied by BDH and purified by recrystallization from acetone (99%), which is polymer non-solvent used in the fractional precipitation process and supplied by RDH. *p*-toluene sulfonic acid ($\geq 98.5\%$), supplied by Sigma-Aldrich, was used as catalyst for esterification step. Besides, it was recovered through dehydration with toluene using Dean-Stark apparatus in order to azeotrope off the water at toluene boiling point. Ceric ammonium nitrate ($\geq 98.5\%$) was supplied from Fluka and used as redox initiator. Toluene ($\geq 99.5\%$), tearic acid (octadecanoic acid) (99%), pyridine, and potassium hydroxide were also supplied by Fluka. Other chemicals include octanoic acid (99%), *cis*-2-butene-1, 4-diol (97%), and nitric acid (70%) were supplied from Merck, Sigma-Aldrich, and Alaph Chemika, respectively, and used without further purification.

Instruments

FTIR spectra of all samples were recorded within wavenumber of 400-4000 cm^{-1} using JSCO FTIR 4200. ^1H -NMR spectrum was recorded on 400 MHz by Bruker Avance 400 spectrometer using deuterated methyl sulfoxide- d_6 (DMSO-d_6) as solvent. GPC with RI detector of Waters BreezeTM 2 HPLC system and THF as eluent was used to determine molecular weight and some associated characteristics of the copolymer. The measurement was carried out using sample flowrate of 1 mL/min and sample volume of 100 μL at 25°C. Shimadzu, DSC-60 analyzer, was used for studying kinetic and thermal characterizations of obtained copolymers. The heating rate was 10 $^{\circ}\text{C}/\text{min}$ under dynamic atmosphere of N_2 at flow rate of 20 mL/min and TGA/DTG curves were obtained using Shimadzu thermogravimetric analyzer TGA-50. The heating rate and N_2 flow rate were 30 $^{\circ}\text{C}/\text{min}$ and 30 mL/min, respectively.

Methods

Synthesis of poly(acrylamide-co-cis-2-butene-1,4-diol)

Acrylamide and *cis*-2-butene-1, 4-diol were dissolved in 3 mL of deionized water and charged into 100 mL one-neck round bottom flask. The CAN solution was prepared by dissolving 1.35 g of ceric ammonium nitrate in 50 mL of 0.5 N of warmed diluted nitric acid, and then it was injected to the flask containing the pre-heated monomers solution (50°C). The polymerization reaction was carried out thermally and ultrasonically in different time of period, in dark and under argon atmosphere. Then, the mixture allowed to cool down to 10°C and poured into a large volume of acetone. The product of white solid powder was filtered, recrystallized using solvent/non-solvent method of water and acetone, washed with acetone two times, and dried in vacuum at room temperature for 24 hours [23,24]. The amounts of monomers and

redox initiator, conditions of polymerization and polymer yields are presented in Table 1.

Esterification of poly (acrylamide-co-cis-2-butene-1, 4-diol)

A mixture of poly(acrylamide-co-cis-2-butene-1,4-diol) PAM-co-C2BDOL (T9 sample), linear aliphatic carboxylic acid, and para toluene sulfonic acid were charged into three-neck round bottom flask equipped with a simple distillation apparatus. The amounts of mixture components are summarized in Table 2. First, the reaction was carried out as homogenous melt between 90 and 100°C with stirrer under argon. Afterwards, it was taken place under vacuum to remove residual water. The product was recrystallized from acetone, washed with acetone three times, and dried at room temperature for 24 hours [25,26].

Hydroxyl number determination

Table 1. Amount of mixture components, polymerization conditions and yields of obtained copolymer

Sample No.	Acrylamide g (mmol)	cis-2-butene-1,4-diol g (mmol)	Ce(NH ₄) ₂ (NO ₃) ₆ (mL)	Reaction time (h)	Temperature (°C)	Ultrasonic	Yield (%)
T1	0.69 (9.8×10 ⁻³)	1.73 (19.6×10 ⁻³)	6	2	50	-	23.9
T2	1.38 (19.6×10 ⁻³)	1.73 (19.6×10 ⁻³)	6	2	50	-	46.1
T3	1.71 (2.4×10 ⁻³)	1.73 (19.6×10 ⁻³)	6	2	50	-	53.6
T4	2.07 (29.5×10 ⁻³)	1.73 (19.6×10 ⁻³)	6	2	50	-	51.4
T5	1.71 (2.4×10 ⁻³)	2.15 (2.4×10 ⁻³)	6	2	50	-	36.7
T6	1.71 (2.4×10 ⁻³)	1.73 (19.6×10 ⁻³)	8	2	50	-	56.6
T7	1.71 (2.4×10 ⁻³)	1.73 (19.6×10 ⁻³)	10	2	50	-	39.8
T8	1.71 (2.4×10 ⁻³)	1.73 (19.6×10 ⁻³)	8	4	50	-	59.7
T9	1.71 (2.4×10 ⁻³)	1.73 (19.6×10 ⁻³)	8	6	50	-	65.1
T10	1.71 (2.4×10 ⁻³)	1.73 (19.6×10 ⁻³)	8	6	65	-	57.4
T11	1.71 (2.4×10 ⁻³)	1.73 (19.6×10 ⁻³)	8	24	50	-	66.2
T12	1.71 (2.4×10 ⁻³)	1.73 (19.6×10 ⁻³)	8	2	25	40 kHz	42.6
T13	1.71 (2.4×10 ⁻³)	1.73 (19.6×10 ⁻³)	8	4	50	40 KHz	60.1
T14	1.71 (2.4×10 ⁻³)	1.73 (19.6×10 ⁻³)	8	6	50	40 KHz	64.7

Hydroxyl number is related to free hydroxyl groups present in polymer chain and determined using ASTM E222 standard test method [27], which involves acetylation of 1g copolymer with 25 mL of acetylation reagent (solution of 21 mL acetic anhydride and 200 mL pyridine) at reflux temperature for 90 min. This can be conducted by using reflux apparatus.

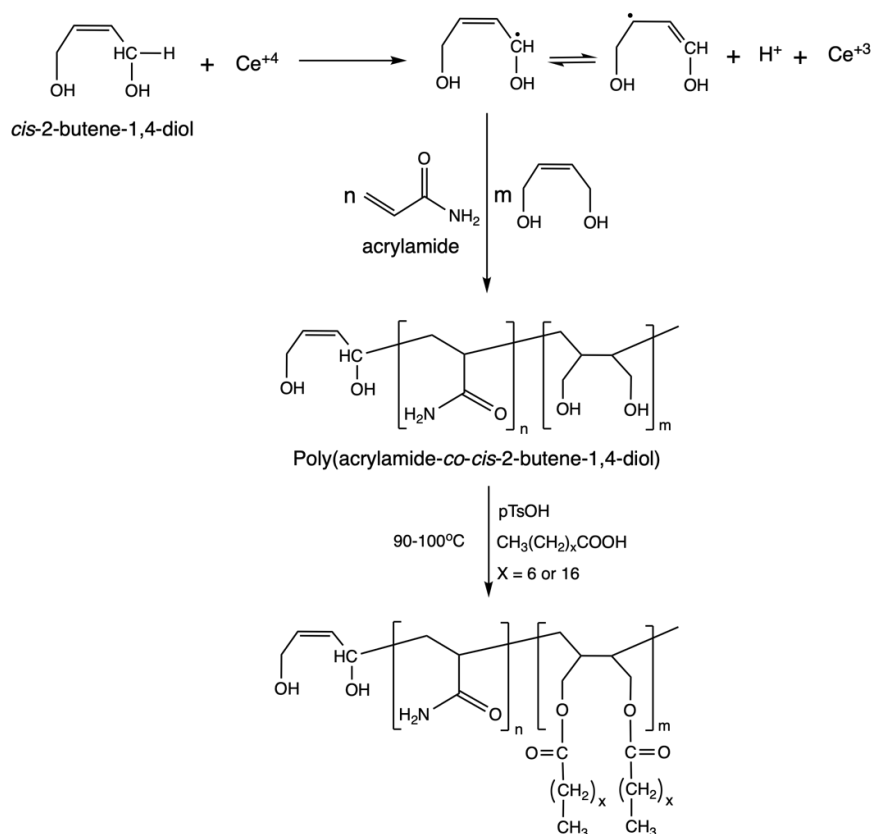
After that, 0.5 mL of phenolphthalein indicator was added to the sample and allowed to titrate with the 0.5 N KOH solution. This method is also performed without adding polymer. The hydroxy number can be calculated as follows:

$$\text{Hydroxyl number} = \frac{(A-B) \times N_t \times 56.1}{W} \quad (1)$$

Where, *A* is KOH volume (mL) required for titration of the blank, *B* is KOH volume (mL) required for titration of the sample, *N_t* is normality of the solution, and *W* is sample weight.

Table 2. The relative amount by weight of PAM-*co*-C2BDOL (T9) and aliphatic carboxylic acids in reaction medium using 1% para toluene sulfonic acid

Sample No.	Aliphatic carboxylic acid	Percentage carboxylic acid by weight (w/w %)	Yield (%)
T12	Octanoic acid	25	72.5
T13	Octanoic acid	50	75.7
T14	Octanoic acid	75	61.3
T15	Stearic acid	25	65.8
T16	Stearic acid	50	69.9
T17	Stearic acid	75	55.1

**Scheme 1.** Chemical equations for synthesis of PAM-*co*-C2BDOL and its esterified formula with octanoic acid and stearic acid.

Results and Discussion

[Scheme 1](#) illustrates a schematic diagram of the expected redox polymerization and esterification mechanism in present study. The general mechanism of polymerization using redox initiator system such as CAN has been defined in some literatures [28,29] and proceeds in several steps: redox initiation, propagation, and termination. In a redox initiation, some

monomers of *cis*-2-butene-1,4-diol undergo initiation and produce free radicals by proton removal from carbon attached with hydroxyl group and then, electron transfer from the extracted proton to the oxidizing agent Ce(IV). During propagation, additional monomer units of both acrylamide and *cis*-2-butene-1, 4-diol are added to the initiated monomer species. High molar ratio of *cis*-2-butene-1, 4-diol, compared to Ce (VI), makes Ce (VI) much more likely react

with *cis*-2-butene-1,4-diol than with remaining active sites in the end of copolymer chains. Termination step involves recombination and disproportionation. In the esterification step, a reaction takes place by nucleophilic attack of hydroxyl groups that attached to copolymer backbone to the carbonyls of aliphatic carboxylic acid.

The percentage of reaction mixture affects polymerization yields, as seen in Table 1. Adding equimolar monomers results in copolymer yield of 46.1% when using 6 mL of CAN solution. A better yield obtained when acrylamide and *cis*-2-butene-1, 4-diol in a ratio of 1.25:1. Likewise, there was a noticeable improvement in yield after adding another 2 mL of CAN solution with the yield increasing 65.1%. Adding more than 8 mL of CAN solution results in lower polymerization yields. Furthermore, the amount of polymer product generally depends on time and this can be clearly seen when polymerization performed for 24 hours, about 66.2% at 50°C and

8 mL of CAN solution. Many articles reported that redox polymerization with CAN performed at temperature between 35-55 °C [30,31]. In the current study, no visible improvement was observed in the yield when temperature exceeded 50°C, up to 65°C, and insignificant yield when temperature is 25°C even when the mixture is subjected to the ultrasonic waves of 40 KHz. However, using a sonochemical method, a slight improvement in yield can be notice.

Characterization

FT-IR analysis

Figure 1 shows the FTIR spectra of PAM-*co*-C2BDOL (T9 sample), esterified PAM-*co*-C2BDOL with octanoic acid and there corresponding monomers. The *cis*-2-butene-1, 4-diol is an aliphatic compound containing a double bond (C=C) which shows absorption band at 1640 cm⁻¹. Band at 3022 cm⁻¹ is assigned to stretching

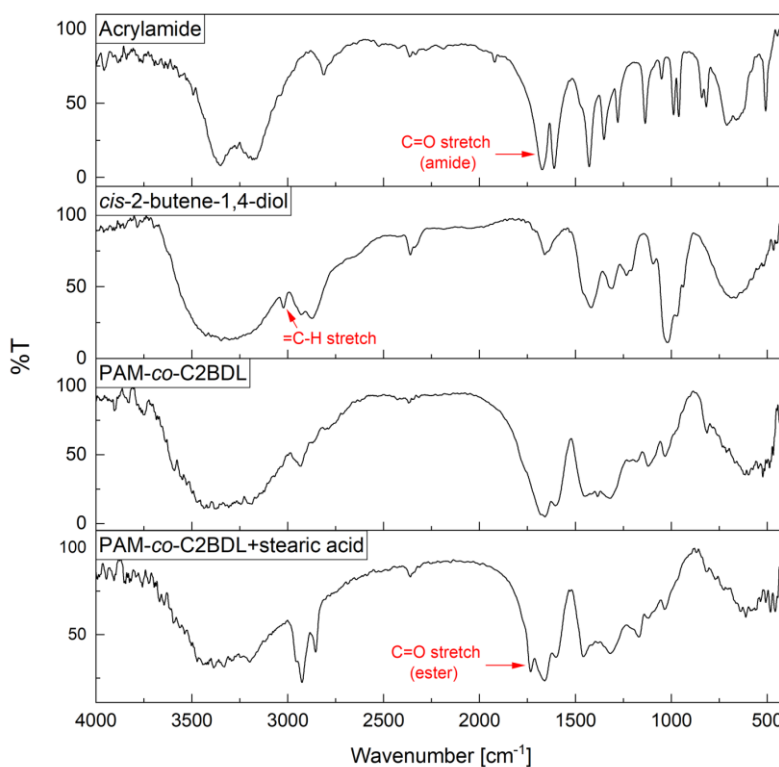


Figure 1. FT-IR of PAM-*co*-C2BDOL, PAM-*co*-C2BDOL+Octanoic acid, and its corresponding monomers.

adjacent bonds ($=C-H$). The broad band between 3150 cm^{-1} and 3600 cm^{-1} is related to hydroxy groups ($O-H$) stretching. Methylene group (CH_2) appears at 2930 cm^{-1} and 2873 cm^{-1} as a result of symmetric and asymmetric bonds stretching, respectively. Acrylamide shows four characteristics absorption bands; two bands at 3349 cm^{-1} and 3185 cm^{-1} assigned to ($N-H$) bonds stretching of amino group, band at 1611 cm^{-1} assigned to ($N-H$) bonds bending, strong band at 1672 cm^{-1} related to ($C=O$) stretching of carbonyl group [32]. It is notable that $C=C$ bond stretching appears within the region of ($C=O$) stretching of carbonyl group. The FTIR of poly(acrylamide-*co-cis*-2-butene-1,4-diol) indicated existence of all bands related to hydroxyl and amide groups. The absences of absorption band at 3040 cm^{-1} assigned to ($=C-H$) bond stretching confirms the success of the copolymerization by redox initiator (Ce^{+4}). The esterified poly(acrylamide-*co-cis*-2-butene-1,4-diol) spectrum indicated appearance of three new bands; a strong band at 1732 cm^{-1} assigned to carbonyl ($C=O$) stretching of formed ester group and the two bands at 1168 cm^{-1} and 1290 cm^{-1} also related to ($C-O$) formed ester group [33], and this confirms the esterification of

poly(acrylamide-*co-cis*-2-butene-1,4-diol) was achieved by nucleophilic attack of hydroxyl groups containing copolymer to carbonyl of octanoic acid and this also confirms the validity of the proposed reaction scheme.

¹H-NMR analysis

¹H-NMR spectra of PAM-*co*-C2BDOL copolymer and esterified formula are depicted in Figure 2. A copolymer spectrum, Figure 2a, indicates signal peaked at 1.4 ppm assigned to protons of methylene groups (a). The adjacent protons (b) of methene groups constituted backbone of copolymer appears a signal peaked at 2.2 ppm. While other adjacent protons (c) of methene groups indicate signal at 1.6 ppm. Due to de-shielding of electron density caused by neighbor hydroxy groups, protons (d) of methene groups have almost same chemical environment and show a signal at higher chemical shift, at 3.5 ppm. The signal at 3.7 ppm is related to the protons (e) of hydroxy groups. Protons (f) of amin groups have a much higher electron de-shielding. They recorded a multiple peaked between 6.8 and 7.2 ppm [34,35]. The ¹H-NMR of esterified copolymer, Figure 2b, shows some differences.

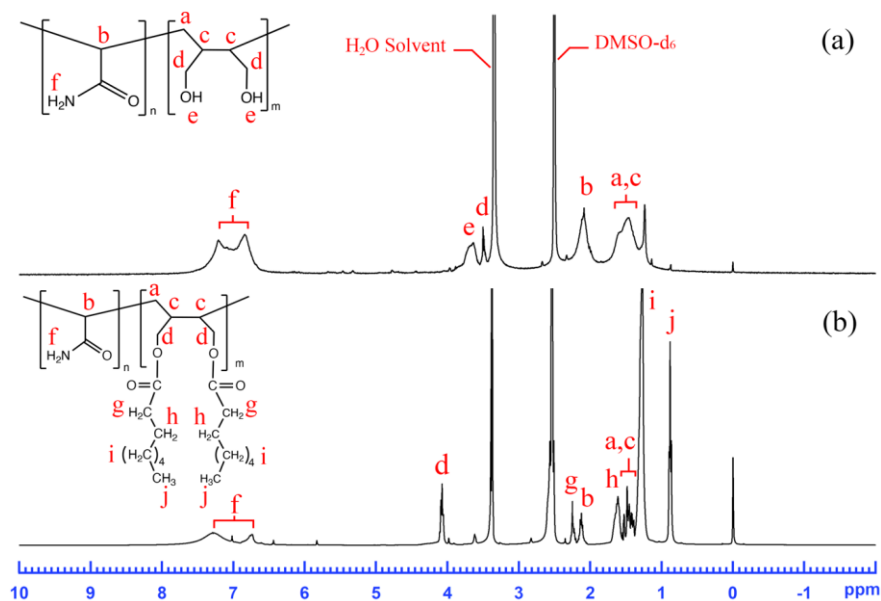


Figure 2. ¹H-NMR spectra (a) PAM-*co*-C2BDOL, (b) esterified copolymer (PAM-*co*-C2BDOL+Octanoic acid).

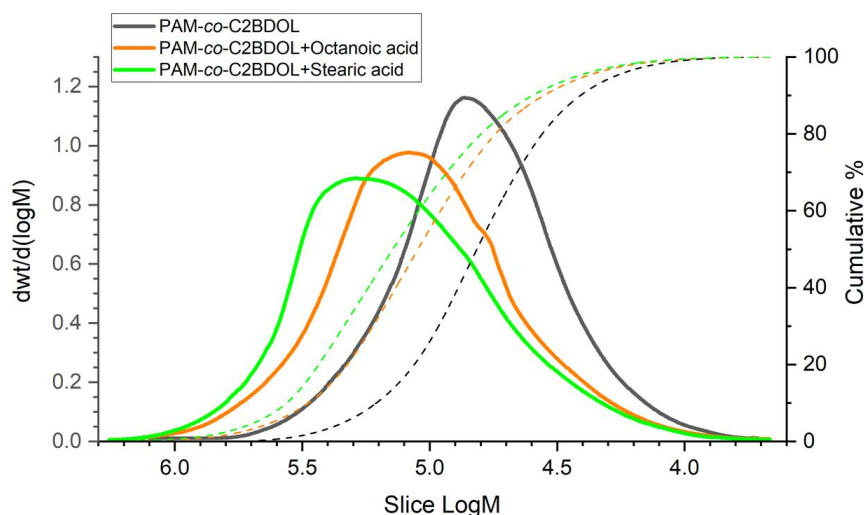


Figure 3. GPC curves of obtained copolymers.

Signals at 2.3 ppm, 1.6 ppm, 1.3 ppm, and 2.3 ppm related to protons (g), protons (h), proton (i), and protons (j), respectively, of methyl and methylene groups that constituted aliphatic branches. Furthermore, there is an obvious decrease in protons (e) signal. That means there is some free hydroxy groups are still intact within copolymer chains. Many literatures reported that esterification process involves absence or decrease of protons (d) signal and deshielding of protons (d) signal to 4.1 ppm [36].

GPC analysis and hydroxyl value calculations

The line curves in Figure 3 represent GPC analysis of resulting copolymer; PAM-co-C2BDOL, PAM-co-C2BDOL+Octanoic acid, and PAM-co-C2BDOL+Stearic acid, while the dashed curves are their cumulative percentages. The former has number average molecular weight (M_n) of 47336 g/mol. With aid of hydroxyl value calculations, the average number of hydroxyl groups in each single chain was nearly 247 and monomers incorporated in copolymer structure is about 77% acrylamide and 23% *cis*-2-butene-1,4-diol. Other related characteristics include weight average molecular weight (M_w), Polydispersity index (PDI) are listed in Table 3.

Esterification of copolymer add long aliphatic chains and more molecular weights to copolymer. This is clearly seen in the GPC curves of both esterified copolymers which indicated number average molecular weight of 84768 g/mol and 92151 g/mol for PAM-co-C2BDOL+Octanoic acid and PAM-co-C2BDOL+Stearic acid, respectively. Esterification of copolymer and octanoic acid showed that around 80% of hydroxyl groups containing copolymer involved in esterification reaction. While, lower percentage of hydroxyl groups contributed in esterification reaction in presence of stearic acid, nearly 69%. This may due to increase of steric hindrance as reactants have larger spatial size [37]. This also reflects on PID of resulting copolymers in which the latest has boarder curve and boarder PID than others, about 1.98.

TGA, DTG, and DSC analysis

The thermal properties of PAM-co-C2BDOL (T9 sample) and its esterified formula with octanoic acid and stearic acid were investigated and depicted in Figure 4, which shows DSC & TGA line graphs at temperatures ranging from 35 °C to 400 °C for DSC and from 35 °C to 600 °C for TGA. Thermal decomposition for PAM-co-C2BDOL, Figure 4a, showed four distant stages of

Table 3. Copolymers molecular weight characteristics obtained from GPC curves

Sample name & No.	M_n (g/mol)	M_w (g/mol)	M_z (g/mol)	PID
PAM-co-C2BDOL (T9)	47336	82108	141614	1.73
PAM-co-C2BDOL+Octanoic acid (T14)	84768	157310	294244	1.85
PAM-co-C2BDOL+Stearic acid (T16)	92151	182827	329339	1.98

weight loss. In the first stage, a slight weight loss at 80 °C is due to removal of moisture and this corresponds to indicating a broad endothermic peak in DSC curve. DSC analysis Indicates occurrence of endothermic transition around 178 °C prior the second stage of mass loss related to glass transition.

The second stage of weight loss was started above 195 °C and ended with copolymer weight loss of 19.76%. This event is an endothermic reaction peaked at 265 °C and it may be due to undergo irreversible intra- and inter- molecular etherification reaction at the hydroxyl groups and imidization reactions at the amide groups with the release of NH_3 , H_2O and minor quantities of CO_2 [38]. In the third and the fourth stages, a major thermal decomposition of copolymer, about 34% mass loss, started around 320 °C with T_{max} of 342 °C. This also combined with a strong peak of exothermic reaction. Some literatures ascribe this reaction to thermal degradation of copolymer backbone [28,39]. The esterified copolymers exhibited some different thermal tends, as shown in Figure 4b and c, which there is multiple stages of weight loss above 150 °C. Introducing ester alkyls as appended groups to copolymer via esterification process can reduce glass transition temperature (T_g) to around 101 °C and 109 °C for octanyl ester copolymer and stearyl ester copolymers, respectively. The overall hydrogen bonding network was weakened due to the existence of ester groups. Prescence of hydrogen bonding network leads to make the forces that holding the chains together stronger [40]. For that same reason, initiating of the second and the third staged of thermal decomposition were taken place at lower temperatures, compared with un-esterified copolymer, around 160 °C and 270 °C,

respectively, and this combined with two endothermic peaks in DSC curve and this may also due to reaction between amide, hydroxyl, and ester groups. Almost half of the alkyl ester copolymer is decomposed in the fourth and the fifth stages. This may attribute to thermal degradation of alkyl ester branches as well as backbone chain which they make up most of copolymer. This comes in good agreement with some literatures [41,42]. The result suggested that the heat resistance of alkyl ester copolymer showed some improvement less than 340 °C. However, this can also affect in increasing the copolymer weight loss above 340 °C, lowering in T_g and lowering in T_{max} in a minimal extent, about 14 °C and 17 °C for octanyl ester copolymer and stearyl ester copolymers, respectively.

Kinetics of thermal decomposition

The Coats–Redfern model is solid-state decomposition used in determining the activation energy and frequency factor through different reaction models, as giving in Table 4. These are model-fitting mainly based on a one-step kinetic equation, giving the following equation [43-45].

$$\ln \left(\frac{g(x)}{T^2} \right) = \ln \frac{AR}{\beta E_a} - \frac{E_a}{RT} \quad (2)$$

Where, R is gas constant, T is temperature in Kelvin, β is heating rate, E_a and A are activation energy and frequency factor of thermal decomposition which directly determined from slope and intercept at Y axis of plot $g(x)$ against $1000/T$, respectively, and α is degree of conversion in the thermal decomposition process, as described in Equation 3.

$$\alpha = \frac{m_o - m_t}{m_o - m_f} \quad (3)$$

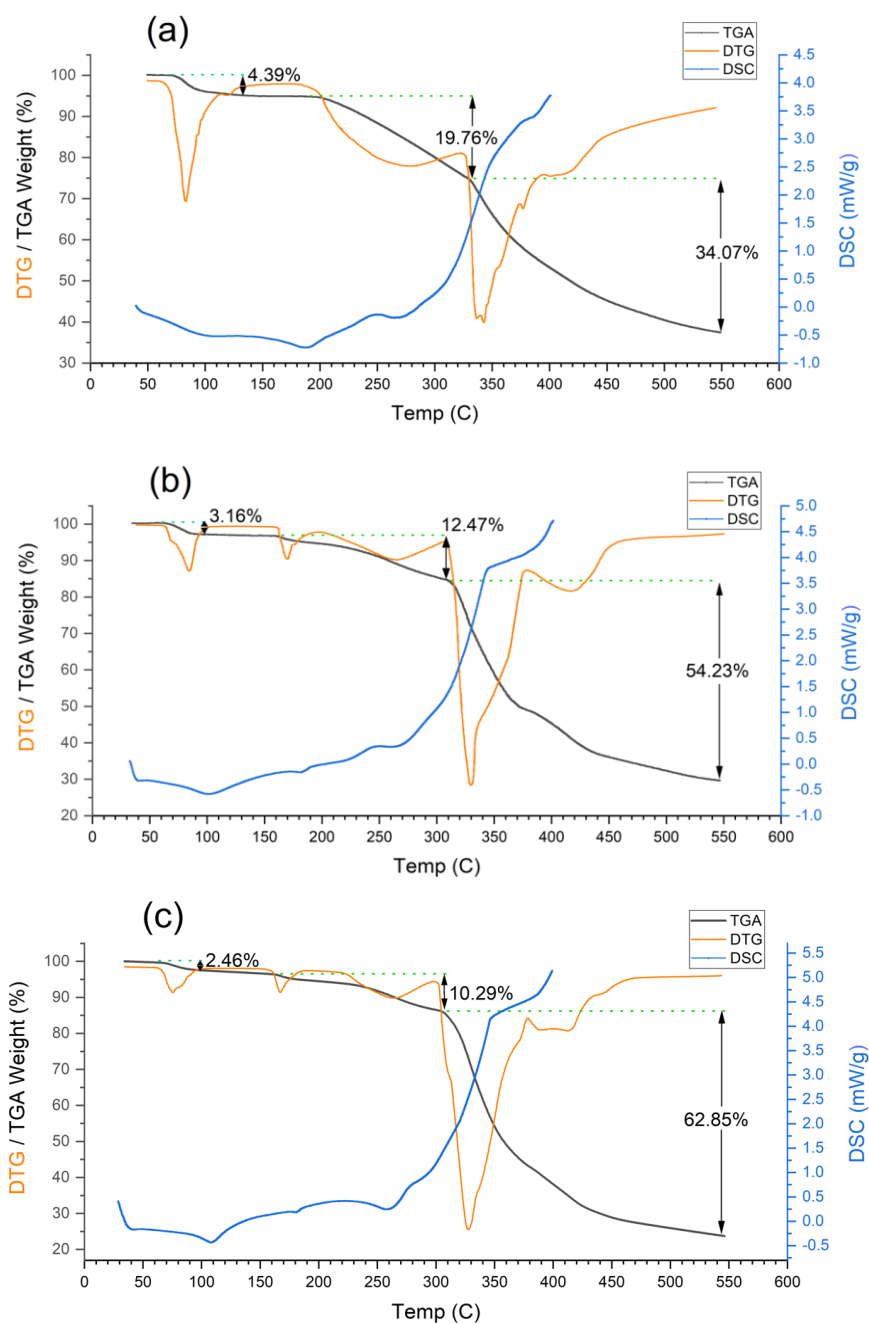


Figure 4. TAG, DTG and DSC analysis of (a) PAM-co-C2BDOL, (b) PAM-co-C2BDOL+Octanoic acid, and (c) PAM-co-C2BDOL+Stearic acid.

Table 4. Chemical reaction models for thermal decomposition used for determination of E_a in current study

Mode name	$g(x)$
The first order	$-\ln(1-\alpha)$
The second order	$(1-\alpha)^{-1}-1$
One dimensional diffusion	α^2
Diffusion control (Janders)	$[1-(1-\alpha)^{1/3}]^2$
Diffusion control (Crank)	$1-(2/3) \alpha-(1-\alpha)^{2/3}$
Contracting cylinder	$1-(1-\alpha)^{1/2}$
Contracting sphere	$1-(1-\alpha)^{1/3}$

Table 4. Chemical reaction models for thermal decomposition used for determination of E_a in current study

Mode name	$g(x)$
The first order	$-\ln(1-\alpha)$
The second order	$(1-\alpha)^{-1-1}$
One dimensional diffusion	α^2
Diffusion control (Janders)	$[1-(1-\alpha)^{1/3}]^2$
Diffusion control (Crank)	$1-(2/3) \alpha-(1-\alpha)^{2/3}$
Contracting cylinder	$1-(1-\alpha)^{1/2}$
Contracting sphere	$1-(1-\alpha)^{1/3}$

Table 5. Activation energies and R^2 correlation of chemical reaction models for thermal decomposition of copolymers, the heating rate is 30 °C /min

Sample name	The first order		The second order		One dimensional diffusion		Diffusion control (Janders)		Diffusion control (Crank)		Contracting cylinder		Contracting sphere	
	E_k (KJ/mol)	R^2 (%)	E_k (KJ/mol)	R^2 (%)	E_k (KJ/mol)	R^2 (%)	E_k (KJ/mol)	R^2 (%)	E_k (KJ/mol)	R^2 (%)	E_k (KJ/mol)	R^2 (%)	E_k (KJ/mol)	R^2 (%)
PAM-co-C2BDOL	36.731	97.2	61.112	99.1	48.154	95	70.644	97.1	62.26	96.7	26.721	95.3	62.961	95.2
PAM-C2BDOL+Octanoic acid	78.549	97.3	109.94	99.3	117.55	94.1	149.26	96.9	137.77	96.2	65.048	95.7	65.33	95.7
PAM-co-C2BDOL+Stearic acid	103.634	98.9	150.89	99.7	146.01	96.8	190.97	98.5	174.43	97.6	84.362	97.9	84.362	97.9

Where, m_o is initial weight of sample, m_t is sample weight at any given temperature, and m_f is final weight of sample after decomposition complete. The results vary and are given in Table 5. All the correlation coefficients of the copolymers are all above 90%, which means the curves fitting the data well [46]. Typical Coats-Redfern models for tested copolymers are following second order near the maximum decomposition temperature in the fourth stage of weight loss and fitted to the experimental data with high R^2 correlation up to 99.7%, which confirms the validity of chosen second order model. This also can be depicted as plot in Figure 5 which the straight lines represent linear fit by the second order. The slope can be used to calculate activation energies. The PAM-co-C2BDOL shows E_a of 61.112 KJ/mol ($R^2=99.1\%$). Adding ester alkyl groups to copolymer chains

shows noticeable increasing in activation energies and this has significant effect on increase the thermal stability of copolymer under elevated temperature. It can be also seen that E_a of PAM-co-C2BDOL+Stearic acid is 150.89 KJ/mol ($R^2 = 99.7$) and higher than PAM-co-C2BDOL+Octanoic acid. This may due to aliphatic side-chains in which stearyl ester groups has twice carbon atoms of octanyl ester group.

Conclusion

In this study, copolymers of (acrylamide-co-cis-2-butene-1, 4-diol) containing alkyl esters as branches were successfully synthesized. Manipulating the concentrations of reactants, initiator, and reaction conditions can optimize yields of poly (acrylamide-co-cis-2-butene-1, 4-diol), octanoyl ester copolymer, and

octadecanoyl ester copolymer up to 65.1%, 75.7%, and 69.9%, respectively. Characterization of those copolymers was performed using FTIR and $^1\text{H-NMR}$, which improved copolymerization of acrylamide and *cis*-2-butene-1,4-diol monomers. Moreover, analyses have also demonstrated that esterification reaction of alkyl acids and poly (acrylamide-*co*-*cis*-2-butene-1,4-diol) was accomplished through nucleophilic attack of copolymer hydroxyl alcohols to carboxylic acid groups of aliphatic acids. Determination of molecular weight by GPC analysis and hydroxyl number by acid-base titration showed that redox polymerization by CAN gives copolymer with a good PDI and contains about 77% acrylamide and 23% *cis*-2-butene-1, 4-diol. In addition, 80% of total hydroxyl groups involved in esterification reaction with octanoic acid, while lower percentage reacted with stearic acid, about 69%. TGA data reveals that copolymer thermal degradation proceeds in four steps of weight loss. Adding alkyl ester to copolymer can affect thermal stability. Thermal degradation steps increased to five steps and the weight loss was enhanced below 340°C. Results also showed that alkyl ester groups increase aliphatic contains in copolymer which has also the potential effect for increasing weigh loss percentage at T_{max} . DSC analysis showed that alkyl esters are soft segments which have a lower T_g than their corresponding copolymers. Kinetics analysis of thermal decomposition using model-fit methods was conducted to explore E_a at the region of T_{max} . Most models showed good R^2 correlation and the second order model is more valid than others with $R^2 = 99.7\%$. The model revealed that E_a generally increased with an increase in the size of linear aliphatic alkyl ester group.

Conflict of interest


The authors declares that there is no conflict of interest in this study.


Orcid

Mahir A. Jalal : 0000-0002-1748-7930

Enas A. Nasir : 0000-0002-2353-1264

Zainab J. Sweah : 0000-0001-8875-8550

Alyaa Abdulhasan Abdulkarem : 0000-0003-0160-5469

Haider Abdulelah : 0000-0002-1530-8687

References

- [1] Y. Liu, H. Xu, L. Zhou, J. Zhang, Highly efficient grafting of polyvinyl acetate onto cellulose nanocrystals in the aqueous phase, *Green Chemistry*, **2023**, 25, 3027-3033. [[Crossref](#)], [[Google Scholar](#)], [[Publisher](#)]
- [2] D. Kumar, J. Pandey, V. Raj, P. Kumar, A review on the modification of polysaccharide through graft copolymerization for various potential applications, *The Open Medicinal Chemistry Journal*, **2017**, 11, 109. [[Crossref](#)], [[Google Scholar](#)], [[Publisher](#)]
- [3] A.S. Sarac, Redox polymerization, *Progress in Polymer Science*, **1999**, 24, 1149-1204. [[Crossref](#)], [[Google Scholar](#)], [[Publisher](#)]
- [4] H.H. Baek, J.M. Lee, J.E. Cho, J.H. Cho, J.H. Kim, I.W. Cheong, Hydroxypropyl methylcellulose-graft-poly (ethyl acrylate-*co*-methyl methacrylate) particles by resin-fortified emulsion polymerization, *Macromolecular Research*, **2010**, 18, 53-58. [[Crossref](#)], [[Google Scholar](#)], [[Publisher](#)]
- [5] N.N. Mzinyane, H. Chiririwa, A.E. Ofomaja, E.B. Naidoo, Effect of ammonium ceric nitrate as initiator in grafting of acrylic acid onto pine cone powder, *Cellulose Chemistry and Technology*, **2019**, 53, 971-979. [[Google Scholar](#)]
- [6] J.H. Trivedi, H.A. Joshi, H.C. Trivedi, Graft copolymerization of acrylonitrile onto sodium salt of partially carboxymethylated tamarind kernel powder using ceric ammonium nitrate as a photo-initiator in an aqueous medium under ultraviolet-radiation, *macromolecular*

- Symposia, Wiley Online Library, **2021**, 2000227. [[Crossref](#)], [[Google Scholar](#)], [[Publisher](#)]
- [7] S. Jha, R. Malviya, S. Fuloria, S. Sundram, V. Subramaniyan, M. Sekar, P.K. Sharma, S. Chakravarthi, Y.S. Wu, N. Mishra, Characterization of microwave-controlled polyacrylamide graft copolymer of tamarind seed polysaccharide, *Polymers*, **2022**, *14*, 1037. [[Crossref](#)], [[Google Scholar](#)], [[Publisher](#)]
- [8] I.İ. Avcı Yayla, E. Sezer, B. Ustamehmetoğlu, Ultrasound and pressure assisted solid-state polymerization of carbazole, *ChemistrySelect*, **2023**, *8*, e202300188. [[Crossref](#)], [[Google Scholar](#)], [[Publisher](#)]
- [9] C. Yagci, U. Yildiz, Redox polymerization of methyl methacrylate with allyl alcohol 1, 2-butoxylate-block-ethoxylate initiated by Ce (IV)/HNO₃ redox system, *European Polymer Journal*, **2005**, *41*, 177-184. [[Crossref](#)], [[Google Scholar](#)], [[Publisher](#)]
- [10] M. Nadia, D. Timotius, S.K. Wirawan, N.R.E. Putri, Y. Kusumastuti, Optimization of ceric ammonium nitrate and ferrous ammonium sulfate in the synthesis of chitosan-graft-maleic anhydride, *IOP Conference Series: Materials Science and Engineering*, IOP Publishing, **2020**, 012037. [[Crossref](#)], [[Google Scholar](#)], [[Publisher](#)]
- [11] J. Dena-Aguilar, J. Jauregui-Rincon, A. Bonilla-Petriciolet, J. Romero-Garcia, Synthesis and characterization of aminated copolymers of polyacrylonitrile-graft-chitosan and their application for the removal of heavy metals from aqueous solution, *Journal of the Chilean Chemical Society*, **2015**, *60*, 2876-2880. [[Crossref](#)], [[Google Scholar](#)], [[Publisher](#)]
- [12] C. Özeroğlu, S. Erdoğan, Oxidative polymerization of acrylamide in the presence of thioglycolic acid, *Central European Journal of Chemistry*, **2005**, *3*, 705-720. [[Crossref](#)], [[Google Scholar](#)], [[Publisher](#)]
- [13] C. Özeroglu, S. Sezgin, Polymerization of acrylamide initiated with Ce (IV)-and KMnO₄-mercaptosuccinic acid redox systems in acid-aqueous medium, *Express Polym Letters*, **2007**, *1*, 132-141. [[Crossref](#)], [[Google Scholar](#)]
- [14] U.P. Singh, H.R. Bhat, R.K. Singh, Ceric ammonium nitrate (CAN) catalysed expeditious one-pot synthesis of 1, 3-thiazine as IspE kinase inhibitor of Gram-negative bacteria using polyethylene glycol (PEG-400) as an efficient recyclable reaction medium, *Comptes Rendus. Chimie*, **2013**, *16*, 462-468. [[Crossref](#)], [[Google Scholar](#)], [[Publisher](#)]
- [15] G.E. Luckachan, L. Jose, V. Prasad, C. Pillai, Sugar end-capped polyethylene: Ceric ammonium nitrate initiated oxidation and melt phase grafting of glucose onto polyethylene and its microbial degradation, *Polymer Degradation and Stability*, **2006**, *91*, 1484-1494. [[Crossref](#)], [[Google Scholar](#)], [[Publisher](#)]
- [16] E. Kot, R. Saini, L.R. Norman, A. Bismarck, Novel drag-reducing agents for fracturing treatments based on polyacrylamide containing weak labile links in the polymer backbone, *SPE Journal*, **2012**, *17*, 924-930. [[Crossref](#)], [[Google Scholar](#)], [[Publisher](#)]
- [17] T. Song, Q. Feng, T. Schuman, J. Cao, B. Bai, A novel branched polymer gel system with delayed gelation property for conformance control, *SPE Journal*, **2022**, *27*, 105-115. [[Crossref](#)], [[Google Scholar](#)], [[Publisher](#)]
- [18] Y. Tatar, E.A. Güvel, N. Kızılcın, Copolymerization of pyrrole and thienyl end capped cyclohexanone formaldehyde resin with Ce (IV) oxidic dibenzoate, *Procedia-Social and Behavioral Sciences*, **2015**, *195*, 2101-2108. [[Crossref](#)], [[Google Scholar](#)], [[Publisher](#)]
- [19] R.R. Bhosale, R.A.M. Osmani, A.S.A. Lila, E.-S. Khafagy, H.H. Arab, D.V. Gowda, M. Rahamathulla, U. Hani, M. Adnan, H.V. Gangadharappa, Ghatti gum-base graft copolymer: A plausible platform for pH-controlled delivery of antidiabetic drugs, *RSC Advances*, **2021**, *11*, 14871-14882. [[Crossref](#)], [[Google Scholar](#)], [[Publisher](#)]

- [20] E. Czarnecka, J. Nowaczyk, Semi-natural superabsorbents based on starch-g-poly (acrylic acid): Modification, synthesis and application, *Polymers*, **2020**, *12*, 1794. [[Crossref](#)], [[Google Scholar](#)], [[Publisher](#)]
- [21] X. Liu, Y. Wen, J. Qu, X. Geng, B. Chen, B. Wei, B. Wu, S. Yang, H. Zhang, Y. Ni, Improving salt tolerance and thermal stability of cellulose nanofibrils by grafting modification, *Carbohydrate polymers*, **2019**, *211*, 257-265. [[Crossref](#)], [[Google Scholar](#)], [[Publisher](#)]
- [22] E. Yavuz, B.F. Senkal, N. Bicak, Poly (acrylamide) grafts on spherical polyvinyl pyridine resin for removal of mercury from aqueous solutions, *Reactive and Functional Polymers*, **2005**, *65*, 121-125. [[Crossref](#)], [[Google Scholar](#)], [[Publisher](#)]
- [23] A. Bajpai, N. Dixit, Polymerization of acrylamide initiated by hydroxy terminated polybutadiene-ceric ammonium nitrate redox system, *Journal of Macromolecular Science, Part A*, **2008**, *45*, 786-794. [[Crossref](#)], [[Google Scholar](#)], [[Publisher](#)]
- [24] B.A. Masry, A.M. Shahr El-Din, H.A. Al-Aidy, Ceric-ions redox initiating technique for Zirconium and Niobium separation through graft copolymerization of natural polysaccharides, *Separation Science and Technology*, **2022**, *57*, 603-618. [[Crossref](#)], [[Google Scholar](#)], [[Publisher](#)]
- [25] A.S. Amarasekara, U. Ha, N.C. Okorie, Renewable polymers: Synthesis and characterization of poly (levulinic acid-pentaerythritol), *Journal of Polymer Science. Part A: Polymer Chemistry*, **2018**, *56*, 955-958. [[Google Scholar](#)]
- [26] L. Sun, L. Zhu, W. Xue, Z. Zeng, Kinetics of p-toluene-sulfonic acid catalyzed direct esterification of pentaerythritol with acrylic acid for pentaerythritol diacrylate production, *Chemical Engineering Communications*, **2020**, *207*, 331-338. [[Crossref](#)], [[Google Scholar](#)], [[Publisher](#)]
- [27] L.L. Jesus, L.M.S. Murakami, T.d.S.D. Mello, M.F. Diniz, L.M. Silva, E.d.C. Mattos, R.d.C.L. Dutra, Evaluation of techniques for determination of hydroxyl value in materials for different industrial applications, *Journal of Aerospace Technology and Management*, **2019**, *11*, e2019. [[Crossref](#)], [[Google Scholar](#)], [[Publisher](#)]
- [28] H. Arslan, M.S. Eroğlu, B. Hazer, Ceric ion initiation of methyl methacrylate from poly (glycidyl azide)-diol, *European Polymer Journal*, **2001**, *37*, 581-585. [[Crossref](#)], [[Google Scholar](#)], [[Publisher](#)]
- [29] A. Shanmugapriya, R. Ramya, M. Venkatachalam, P. Sudha, Optimization of ceric ammonium nitrate initiated graft copolymerization of acrylonitrile onto chitosan, *Journal of Water Resource and Protection*, **2011**, *2011*. [[Crossref](#)], [[Google Scholar](#)], [[Publisher](#)]
- [30] Y. Song, D. Wei, Preparation and characterization of graft copolymers of silk sericin and methyl methacrylate, *Polymers and Polymer Composites*, **2006**, *14*, 169-174. [[Crossref](#)], [[Google Scholar](#)], [[Publisher](#)]
- [31] A. Mohammed, Studies on graft copolymerization of acrylic acid onto acetylated cellulose from maize cob, *Journal of the Turkish Chemical Society Section A: Chemistry*, **2022**, *9*, 571-578. [[Crossref](#)], [[Google Scholar](#)], [[Publisher](#)]
- [32] R.M. Silverstein, G.C. Bassler, Spectrometric identification of organic compounds, *Journal of Chemical Education*, **1962**, *39*, 546. [[Crossref](#)], [[Google Scholar](#)], [[Publisher](#)]
- [33] M. Worzakowska, TG/FTIR/QMS studies of long chain esters of geraniol, *Journal of Analytical and Applied Pyrolysis*, **2014**, *110*, 181-193. [[Crossref](#)], [[Google Scholar](#)], [[Publisher](#)]
- [34] P.D. Svoronos, CRC handbook of basic tables for chemical analysis: Data-driven methods and interpretation, **2020**. [[Google Scholar](#)], [[Publisher](#)]

- [35] K. Watanabe, H. Matsushita, K. Takamatsu, K. Ute, ¹H DOSY analysis of high molecular weight acrylamide-based copolymer electrolytes using an inverse-geometry diffusion probe, *Polymer Journal*, **2023**, *55*, 591-598. [[Crossref](#)], [[Google Scholar](#)], [[Publisher](#)]
- [36] M. Kwiecień, I. Kwiecień, I. Radecka, V. Kannappan, M.R. Morris, G. Adamus, Biocompatible terpolyesters containing polyhydroxyalkanoate and sebacic acid structural segments—synthesis and characterization, *RSC Advances*, **2017**, *7*, 20469-20479. [[Crossref](#)], [[Google Scholar](#)], [[Publisher](#)]
- [37] G. Odian, Principles of polymerization, *John Wiley & Sons*, **2004**. [[Google Scholar](#)]
- [38] X. Zhang, M. Han, A. Fuseni, A.M. Alsofi, An approach to evaluate polyacrylamide-type polymers' long-term stability under high temperature and high salinity environment, *Journal of Petroleum Science and Engineering*, **2019**, *180*, 518-525. [[Crossref](#)], [[Google Scholar](#)], [[Publisher](#)]
- [39] X. Fu, Q. Yang, Y. Zhang, Thermal decomposition behavior and mechanism study of cationic polyacrylamide, *Journal of Thermal Analysis and Calorimetry*, **2021**, *146*, 1371-1381. [[Crossref](#)], [[Google Scholar](#)], [[Publisher](#)]
- [40] S. Faridi, A. Mobinikhaledi, H. Moghanian, M. Shabanian, Synthesis of novel modified acrylamide copolymers for montmorillonite flocculants in water-based drilling fluid, *BMC Chemistry*, **2023**, *17*, 125. [[Google Scholar](#)], [[Publisher](#)]
- [41] L. Raghunanan, S.S. Narine, Influence of structure on chemical and thermal stability of aliphatic diesters, *The Journal of Physical Chemistry B*, **2013**, *117*, 14754-14762. [[Crossref](#)], [[Google Scholar](#)], [[Publisher](#)]
- [42] Y. Jiang, A.J. Woortman, G.O.A. van Ekenstein, K. Loos, Environmentally benign synthesis of saturated and unsaturated aliphatic polyesters via enzymatic polymerization of biobased monomers derived from renewable resources, *Polymer Chemistry*, **2015**, *6*, 5451-5463. [[Crossref](#)], [[Google Scholar](#)], [[Publisher](#)]
- [43] S.A. Al-Bayaty, R.A. Al-Uqaily, N.J. Jubier, Using the Coats-Redfern method during thermogravimetric analysis and differential scanning calorimetry analysis of the thermal stability of epoxy and epoxy/silica nanoparticle nanocomposites, *Journal of Southwest Jiaotong University*, **2020**, *55*. [[Crossref](#)], [[Google Scholar](#)], [[Publisher](#)]
- [44] S.K. Paswan, S. Kumari, M. Kar, A. Singh, H. Pathak, J. Borah, L. Kumar, Optimization of structure-property relationships in nickel ferrite nanoparticles annealed at different temperature, *Journal of Physics and Chemistry of Solids*, **2021**, *151*, 109928. [[Crossref](#)], [[Google Scholar](#)], [[Publisher](#)]
- [45] B.Y. Li, M.Y. Tee, K.S. Nge, A.K.L. Ng, W.W.F. Chong, J.H. Ng, G.R. Mong, Comparison kinetic analysis between coats-redfern and criado's master plot on pyrolysis of horse manure, *Chemical Engineering Transactions*, **2023**, *106*, 1273-1278. [[Crossref](#)], [[Google Scholar](#)], [[Publisher](#)]
- [46] J. Ge, R.q. Wang, L. Liu, Study on the thermal degradation kinetics of the common wooden boards, *Procedia Engineering*, **2016**, *135*, 72-82. [[Crossref](#)], [[Google Scholar](#)], [[Publisher](#)]

HOW TO CITE THIS ARTICLE

M.A. Jalal, E.A. Nasir, Z.J. Sweah, A.A. Abdulkarem, H. Abdulelah. Synthesis, Characterization and Thermal Properties of Some Acrylamide and *Cis*-2-Butene-1,4-Diol Copolymers Using CAN as Initiator. *Adv. J. Chem. A*, 2025, 8(3), 504-518.

DOI: [10.48309/AJCA.2025.472480.1634](https://doi.org/10.48309/AJCA.2025.472480.1634)

URL: <https://www.ajchem-a.com/article/205443.html>